

**ICAS PAPER**

**No.** 72 - 18



TECHNOLOGICAL ADVANCES IN  
AIRFRAME-PROPULSION INTEGRATION

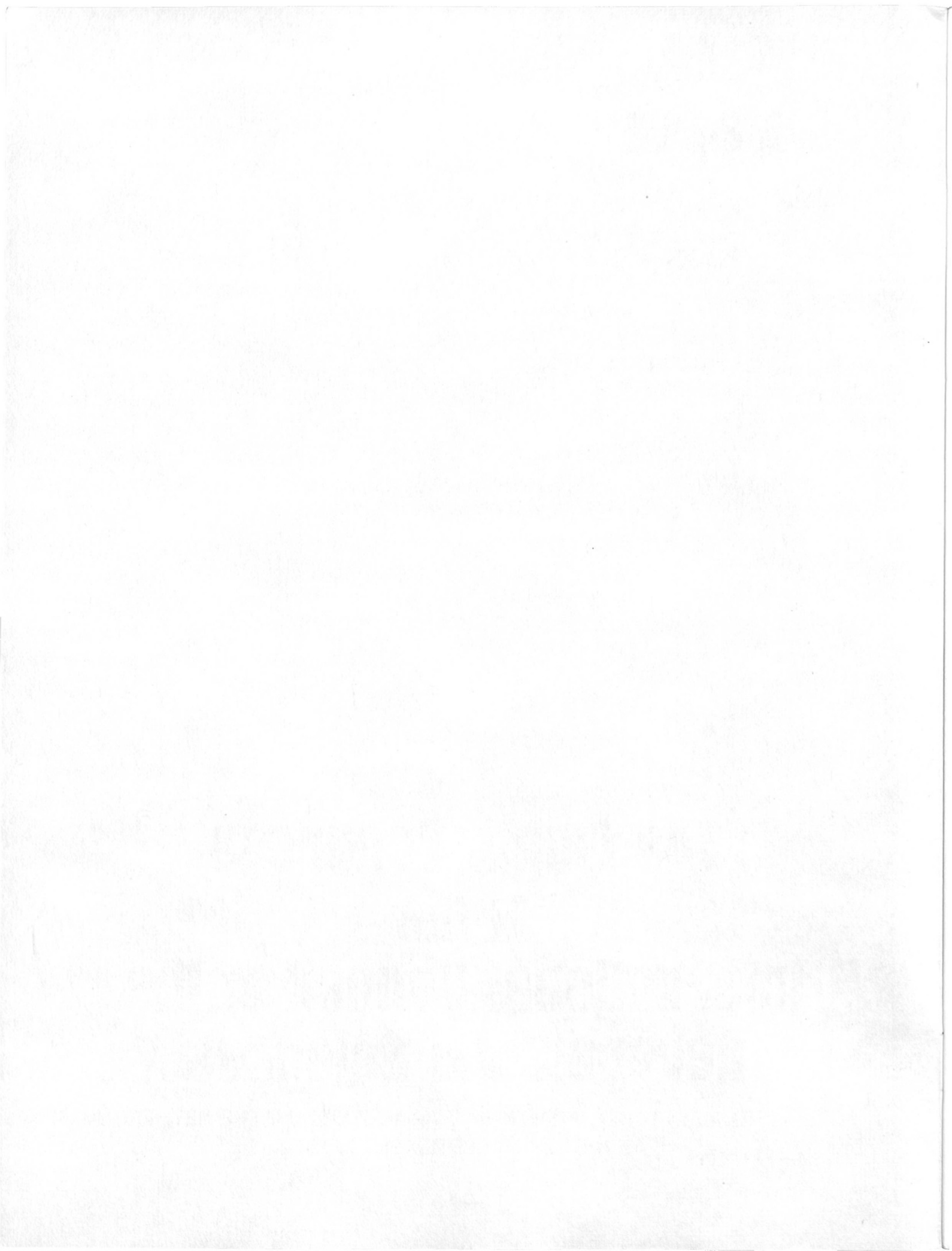
by

Demetrius Zonars, Chief Scientist  
Air Force Flight Dynamics Laboratory  
Wright-Patterson Air Force Base, Ohio USA

**The Eighth Congress  
of the  
International Council of the  
Aeronautical Sciences**

INTERNATIONAAL CONGRESCENTRUM RAI-AMSTERDAM, THE NETHERLANDS  
AUGUST 28 TO SEPTEMBER 2, 1972

Price: 3. Dfl.



## TECHNOLOGICAL ADVANCES IN AIRFRAME-PROPULSION INTEGRATION

D. Zonars, Chief Scientist  
Air Force Flight Dynamics Laboratory  
Air Force Systems Command  
Wright-Patterson Air Force Base, Ohio

### Abstract

F-111A aircraft inlet system and TF-30 engine compatibility is reviewed based on an assessment of time averaged and instantaneous distortion parameters. In addition, recent advances in research on inlet configurations associated with steady-state and dynamic distortions are presented. A complete random data acquisition, editing and processing method is described for accomplishing data analysis as an inlet flow diagnostic tool. Finally, recent afterbody and nozzle research results, which improve the technology base for understanding airframe-nozzle interactions, are reviewed. A basic aircraft configuration incorporating a common forebody, wing, inlet system and a twin engine installation was utilized during high Reynolds number wind tunnel tests to determine the relative merits of a wide spectrum of afterbody-nozzle geometrical variations.

### I. Introduction

Over the past twenty years, both military and civilian flight vehicle sophistication has drastically increased as a result of the ever proliferating demands for improved performance. This increase in aerospace system sophistication has been possible through new and rapidly emerging technologies including the advent of new design techniques and facility testing methods.

The continuing degree of interest displayed in airframe-propulsion integration is not surprising since this technical domain involves critically important influences which strongly impact vehicle performance. More importantly, this area has been under significant scrutiny due to the difficulties experienced in the operation of tactical type aircraft. The most severe problem has been engine surge or compressor stall due to steady-state and dynamic distortion emanating principally from the inlet. On the other hand, acknowledgment of the excessive drag associated with inlet and nozzle installations has been of a subtle nature with low level attention given to this subject until recently. In both cases, variable geometry systems have been employed to accommodate the wide range of mass flow and pressure ratio characteristics required for matching airframe and propulsion systems.

The transonic flight regime still appears as the most difficult portion of the speed range in which limited analysis methods can be applied to predict airframe-nozzle interactions. By necessity, one must turn to experimental means in order to develop a viable and correct determination of the phenomena involved. The AF Flight Dynamics Laboratory has undertaken a number of programs to investigate the effects of air flows about fuselage and fuselage-wing configurations throughout the subsonic, transonic and supersonic speed regimes. A portion of this work is reported herein.

### II. F-111 Inlet Flight Experiences

Advanced tactical aircraft are required to perform a number of missions which demand a high degree of airframe propulsion integration including low flow distortion over a much larger range of operating conditions (Mach number, altitude, angle of attack, engine mass flow) than previous supersonic tactical aircraft systems. Requirements for maneuvering flight in a low drag configuration necessarily implies high angle of attack flight attitudes from subsonic to supersonic speeds in excess of Mach number 2.0.

It has been, therefore, quite natural to utilize an inlet design for the F-111A which takes advantage of the flight vehicle fuselage and wing to reduce the effects of angle of attack and angle of yaw during maneuvering flight. The F-111A inlet shown in Figure 1 is an external compression 88 degree segment of an axisymmetric inlet which is integrated with the airframe fuselage-wing root intersection. Locating the inlet in the wing-fuselage flow field also provides precompression for the inlet flow in supersonic flight which means that the inlet capture area is reduced from that required at free stream conditions. Further, a significant vehicle weight savings is realized by integrating the supporting structure of the inlet and relatively short duct with the vehicle structure.

The spike system of the inlet translates fore and aft and the second cone angle varies with flight Mach number and angle of attack to vary the inlet throat area. Each of the inlets is matched to a Pratt and Whitney TF-30-P-3 afterburning turbofan engine. The modulated afterburner improves the tactical ability of the F-111A by providing a variable thrust output in afterburner mode upon demand by the throttle. Therefore, in addition to being closely integrated with the airframe, the F-111A inlet system is closely integrated with the engine to accommodate variations in airflow demand during engine transient operation.

During prototype flight tests of the F-111A, it became apparent that the desired flight envelope was restricted. Maneuverability of the aircraft at high subsonic speeds and supersonic speeds was being limited by a rapid buildup of steady and dynamic inlet flow distortion resulting in engine compressor stall. This incompatibility of the inlet and engine in the F-111A aircraft was the impetus for a comprehensive evaluation of flight test and wind tunnel data to identify the causes of the compressor stalls and define modifications to the inlet system to reduce the incidence of compressor stalls in both steady state and maneuvering flight.

In order to identify problem areas and suggest modifications to improve the inlet system and its compatibility with the engine, the inlet of a prototype airplane was equipped with diagnostic total and static pressure instrumentation in the inlet and engine. In addition, the engine compressor

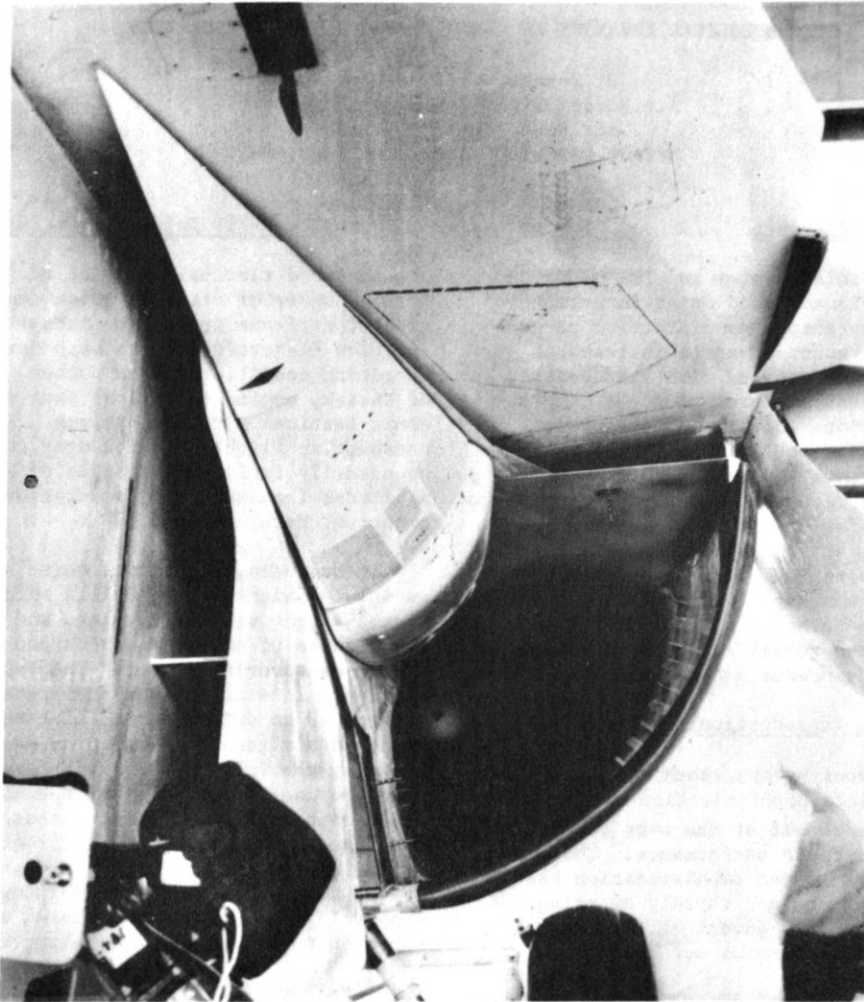


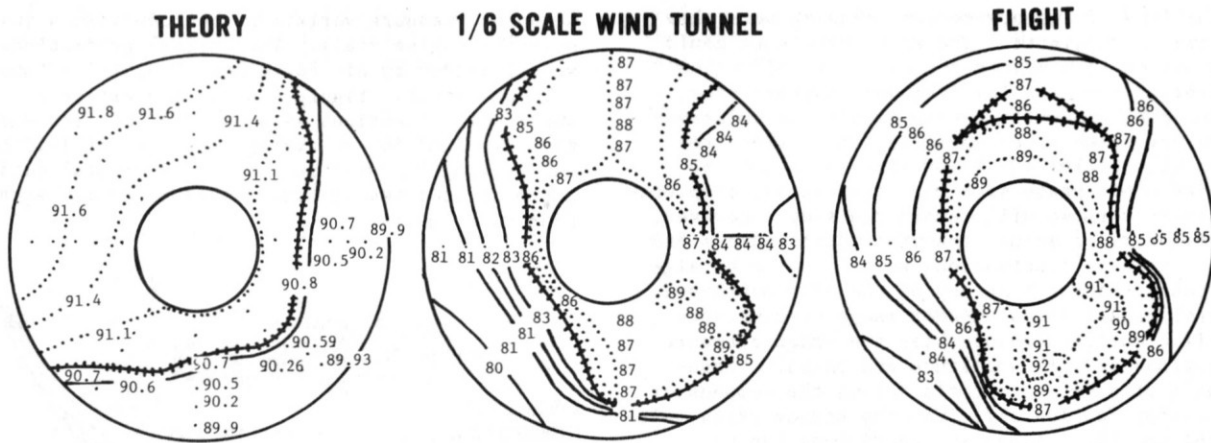
FIGURE 1. AFT VIEW OF TYPICAL F-111A INLET

face was equipped with 40 total pressure probes in centroids of equal areas to map the total pressure pattern entering the fan and low pressure compressor of the engine. There were eight rakes with five probes per rake.

Initially, a theoretical study was undertaken to determine the anticipated steady state distortion at the compressor face during supersonic flight. The purpose of this study was to compare such information with similar 1/6 scale wind tunnel and actual flight test data and thus provide insight as to trouble areas resulting from specific theoretical-experimental differences. The conditions of Mach number 2.2 and angle of attack of 5.5 degrees with an initial inlet cone angle of 12.5 degrees and second cone angle of 24 degrees was chosen. The theoretical approach first consisted of estimating the Mach number aft of the conical wave system resulting from the fuselage-wing glove intersection. This yielded a Mach number of 2.08 wherein the flow field was assumed to be uniform to the inlet. An exact Taylor-Maccoll solution was developed for the initial cone angle with subsequent use of the method of characteristics to generate the flow field about the second cone. A normal shock was then assumed at the entrance to the cowl lip. The resulting isobars for this 88 degree inlet segment were then

uniformly expanded into a circumferential profile at the compressor face. A plane of symmetry was assumed half way between the 88 degree sector of the inlet system. The total pressures resulting from such calculations were plotted and compared with those of the 1/6 scale wind tunnel and flight case. Figure 2 shows such a comparison. The wind tunnel and flight data showed a remarkably similar profile, however the comparison with theory is understandably different due to the absence of viscous effects. More importantly, the main difference stems from a clearly identifiable low energy area on the inboard, lower portion of the compressor face which is quite different than that predicted by the inviscid theory. It was therefore clear that an investigation should be undertaken to survey the oncoming and duct flow relating to this portion of the entire airflow. Values of steady state distortion are also presented as derived from the expression  $K_{DA}$  as follows:

$$K_{DA} = \frac{\sum_{i=1}^5 \left[ \frac{P_{t_{av}} - P_{t_{min}}}{P_{t_{av}}} \right]_i \theta_i^{-1} C_i}{\sum_{i=1}^5 C_i} \times 100 \quad (1)$$



LEFT HAND ENGINE LOOKING AFT

PARAMETER	THEORY	WIND TUNNEL	FLIGHT
AIR FLOW, LBS / SEC.	168	168	162
+++++ AVE. RECOVERY PRESSURE RATIO	90.8	85	87
DISTORTION FACTOR, $K_{DA}$	100	383	428

FIGURE 2. COMPARISON OF F-111A COMPRESSOR FACE TOTAL PRESSURES FOR MACH NUMBER 2.2 and AN ANGLE OF ATTACK OF 5.5 DEGREES

where

$C$  = ratio of compressor inlet radius to ring radius

$i$  = number of ring

$\theta^-$  = largest continuous arc of the ring over which the total pressure is below the ring average pressure

$P_{t_{av}}$  = ring average total pressure

$P_{t_{min}}$  = ring minimum total pressure

Here again, the low theoretical  $K_{DA}$  value is due to the absence of the low, inboard impact pressures and the inviscid assumptions.

In the analysis of the flight test data taken with this instrumentation, several approaches were employed. First, compressor face total pressure maps were compared, which showed the changes in flow distortion as a compressor stall condition was approached. Although this analysis indicated a low total pressure region on the inboard side, the results were inconclusive and so time variations of data from other sets of instrumentation further upstream in the duct were examined for many stall sequences in order to identify problem areas in the inlet flow field as they developed. From the time sequence plots, selected data for a particular time cut were used to define duct static pressure distributions or boundary layer total pressure profiles. The static pressure distributions were used to locate shock wave positions, indicate boundary layer bleed effectiveness, estimate stream velocities, and indicate regions of separated flow. Total pressure profiles were used to define regions of low energy flow ahead of and in the inlet, and

to indicate regions of separated flow. In a parallel study coordinated with this quasi-steady data evaluation, the dynamic pressure fluctuations indicated by traces from the flight telemetry and magnetic tape output of the individual probes were being carefully analyzed. Under certain flight conditions, the traces indicated extreme "turbulence" at the compressor face. This was known to cause a loss in engine stability in other engines as reported by Gabriel, Wallner and Lubick<sup>(1)</sup> and was felt to be a contributory factor in the stall problems of the F-111A. Although a complete correlation between quasi-steady flow distortion and dynamic pressure fluctuations was not undertaken, it was realized that there was a cause and effect relationship between these two types of distortion and the approach was to address the cause of unsteady and non-uniform flow in the inlet and attempt to eliminate it. A corresponding reduction of the severity of the dynamic-pressure fluctuations (dynamic distortion) would be expected, but it was important to know the relationships between steady and dynamic flow to the limits of the instrumentation signal available.

### III. F-111 Inlet Pressure Fluctuation Effects

The effects of transient disturbances, or more specifically, the fluctuating nature of the measured total pressures at the compressor face were considered to have a strong influence in the stall properties of the engine. This influence and corresponding effect were considered to be above the acceptable steady-state distortion which could be accommodated by the engine. The flight regime in which this phenomenon commenced was found to be at low supersonic speeds, with increasing disturbance intensity as a function of increasing Mach number. These disturbances exhibited a wide range

of amplitude-frequency content showing both slow and rapid transients. The slow transients could possibly be compensated for by inlet and engine controls. For such low frequency disturbances, engine performance is basically similar to steady-state operation since normally, the outlet pressures will follow the inlet flow variations in magnitude and phase such that the overall compressor pressure ratio will remain the same. However, the majority of actual transient disturbances and total pressure fluctuations were found to be significantly faster than any of the aforementioned control capabilities. Under these circumstances, specific outlet pressures lag the inlet pressure variations in both amplitude and phase. Consequently, the pressure ratio across the compressor can differ considerably from the steady-state value on the operating line, and conditions can be reached wherein compressor stall margin reduction and even stall will be experienced. Data from reference (1) has shown this to be the case for a simply induced sinusoidal pressure variation input to a compressor.

It is important to note here that the original compressor face total pressure instrumentation on the prototype test aircraft was never intended for the accurate measurement and analysis of transient disturbances. Hence, an effort to correlate transient disturbances with the lower frequency average values of the measured total pressures to the compressor face required special data reduction methods. Total pressure readout from flight magnetic tapes at conditions appropriate to engine stall were first identified and then processed through narrow band pass filters by the Field Measurements Group of the Air Force Flight Dynamics Laboratory. Figure 3 shows two typical frequency spectrums obtained from the filtering process of the flight test data wherein 85.55 inch long pressure carrying lines were provided between the pressure probes and the transducers. At first

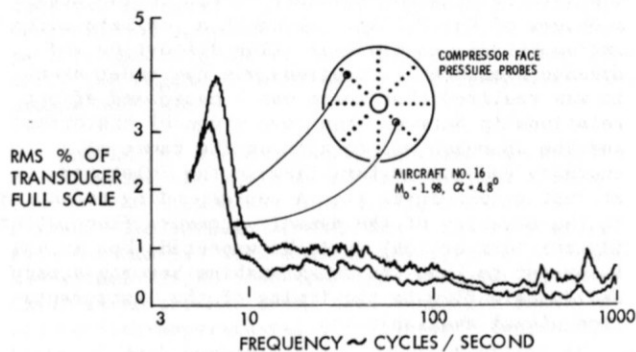


FIGURE 3. TYPICAL F-111A COMPRESSOR FACE PRESSURE AMPLITUDE-FREQUENCY SPECTRUM

glance, the higher amplitude data would appear to occur at the lower frequencies; however, the utilization of 85.55 inch lines (tubulation) for steady state pressure measurements suggested the possibilities of transient signal attenuation to the transducer due to classical acoustic type dissipation. In order to correct for this tubulation effect, an experimental program was undertaken by the Aero-Acoustics Branch of the Air Force Flight Dynamics Laboratory to apply corrections to the

measured pressure variations for conditions just prior to engine stall. Theoretical predictions were provided by Air Force Aero Propulsion Laboratory personnel. Figure 4 shows the nature of the amplitude corrections as a function of frequency when examined for an average pressure of 14.7 psi and varying temperature. The experimental data taken at room temperature showed excellent agreement with theory.

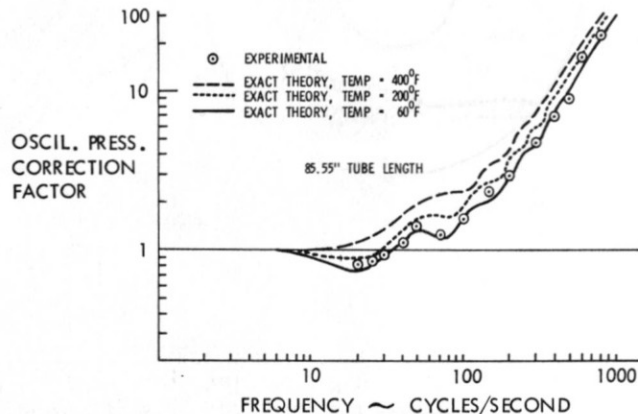


FIGURE 4. F-111A OSCILLATORY PRESSURE TUBULATION CHARACTERISTICS

Many supersonic flight conditions associated with engine stall were examined with specific emphasis on the high frequency aspects of the transient disturbances. Multiplexing of the instrumentation, as is normally accomplished on test aircraft for measuring steady-state parameters, was found to have a strong influence on the high frequency transient data. In an effort to isolate these effects, several flights were performed involving a minimum of multiplexing with a 15 inch line replacing one of the 85.55 inch lines for reduced tubulation effects. A comparison of pressure transients in a 85.55 inch line with multiplexing versus a 15 inch length tubing with minimal multiplexing is shown in Figure 5.

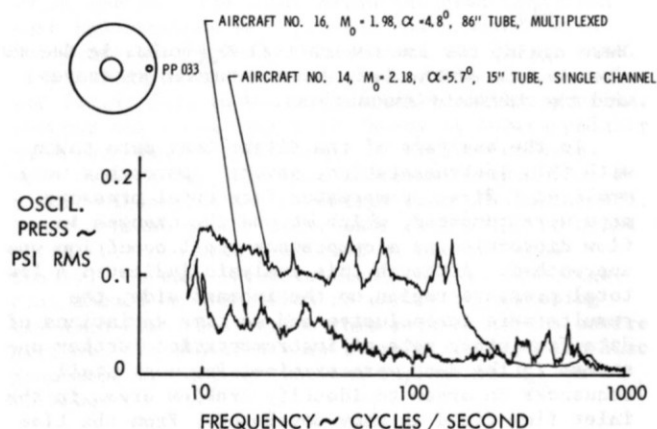


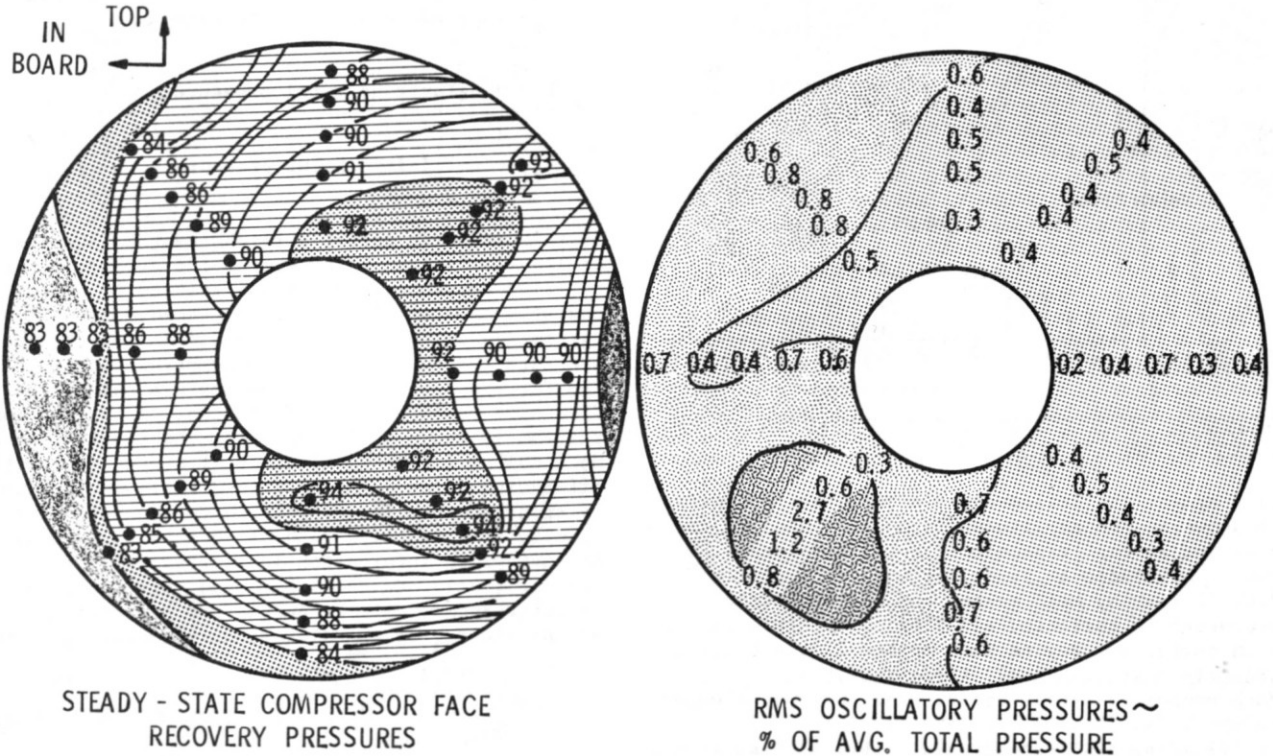
FIGURE 5. COMPARISON OF F-111A TUBULATION

Above approximately 250 cps it can be seen that the high frequency transients recorded with the 85.55 inch line were due to multiplexing, and not present except for some disturbances in the 525-660 cps range. It was, therefore, decided to utilize the

0 - 250 cps frequency range for data analysis when transient data was subject to multiplexing, and 0 - 1000 cps for the data with minimal multiplexing.

A specific comparison of steady-state compressor face recovery pressures with corresponding transient disturbance values obtained from flight is shown in Figure 6. The oscillatory or transient pressure data is based on 0 - 250 cps as discussed above. Figure 6 shows, generally, that the high,

angle of attack on the dynamic characteristics of this probe at a constant  $M_0 = 0.77$ . Although many discrete frequencies were identified from the spectrum analyzer output, specific frequencies of 130, 230, and 525 cps appeared to persist with relatively high amplitude for this test condition, which was at a military power engine setting. The amplitudes of these particular frequencies appeared to be fairly constant up to moderate angle of attack with a tendency to converge and further increase in



AIRCRAFT 16;  $M_0 = 1.98$ ,  $\alpha = 4.8^\circ$ , 0.2 SECONDS BEFORE ENGINE STALL

FIGURE 6. F-111A COMPRESSOR FACE STEADY-STATE AND OSCILLATORY PRESSURES

steady-state recovery pressures corresponded to areas of reduced transient or oscillatory pressures, whereas low recovery pressures related to regions of higher transient values. The region in the lower left-hand corner of the oscillatory pressure map was of particular interest. This area of highest transient disturbance values corresponded directly to the lower left-hand portion of the inlet which was most susceptible to boundary layer ingestion. In addition, the steady-state analysis from flight demonstrated the upward spreading of low total pressures from the bottom of the sharp cowl lip with increasing angle of attack. The data of Figure 6 would indicate that, in addition to being of a very low recovery nature, this portion of the flow possessed a high degree of flow unsteadiness sufficient to cause engine stall.

The transient disturbance analysis for all 40 compressor face pressure measurements for a particular stall condition would have required a prohibited expenditure of manhours and it was, therefore, decided to use an available single pitot tube of 15 inch tubulation to examine the fluctuating nature of the duct flow. Figure 7 shows the effect of

amplitude at higher angles of attack until engine compressor stall was experienced. Also shown on Figure 7 are the effects of first zone afterburner operation for cruise angle of attack. The

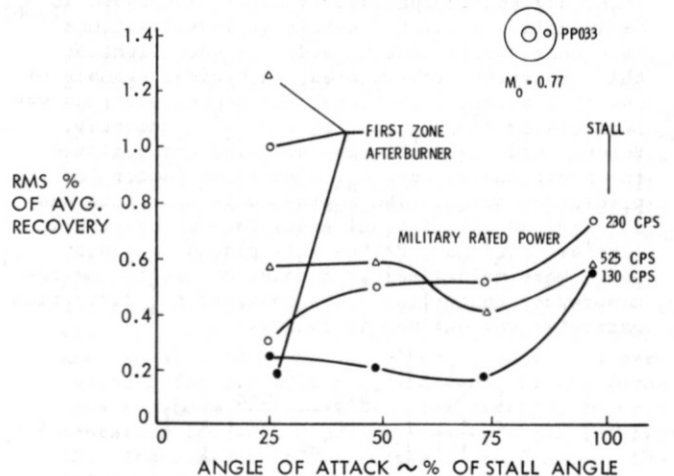


FIGURE 7. F-111A COMPRESSOR FACE PRESSURE FLUCTUATIONS VS. ANGLE OF ATTACK

amplitude associated with 130 cps was found to change a small amount, however, there was a substantial amplitude increase in the 230 and 525 cps frequencies.

The condition of aircraft acceleration for cruise angle of attack at maximum afterburner power was examined with results as presented in Figure 8.

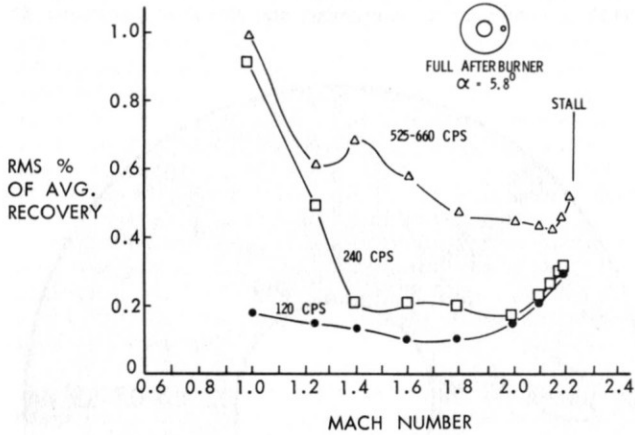


FIGURE 8. F-111A COMPRESSOR FACE PRESSURE FLUCTUATIONS VS. MACH NUMBER

Here again, the influence of afterburner operation is shown in the amplitudes of the 240 and 525 cps frequencies for transonic flight conditions. However, amplitudes at these frequencies decreased with increasing Mach number and corresponding decreases in corrected air flow up to approximately Mach number 2. Beyond Mach number 2, there was a dramatic increase in all three amplitudes up to Mach number 2.2 where engine stall was experienced.

From the quasi-steady and transient disturbance data studied during 1967, it was clear that the engine compressor stall characteristics were strongly influenced by inlet pressure pulsations at high frequencies and this effect must be considered in conjunction with the "steady-state" distortion.

#### IV. Detailed Studies of F-111A Inlet and Engine Air Flow Fluctuation Effects

Subsequent to the initial study of the F-111A inlet engine incompatibility effort discussed in Section III, a limited number of investigations<sup>(2-6)</sup> have been carried out in order to shed light on this important problem area. A typical example of one of the more significant and recent programs was reported by Plourde and Brimelow<sup>(7)</sup>. Recently, Burcham and Hughes<sup>(8)</sup> have modified and utilized the Pratt and Whitney  $K_{DA}$  distortion factor for predicting surge. The engine compressor face was sub-divided into 5 equal areas through concentric circles or rings. Probes were placed on rings which were maintained at a constant radii from the compressor centerline. The modified  $K_{DA}$  distortion parameter was defined as follows:

$$K_{DM} = \frac{\frac{1}{2} \sum_{i=1}^5 \left[ \frac{P_{t \max} - P_{t \min}}{P_{t \text{av}}} \right] \theta_i^- C_i}{\sum_{i=1}^5 C_i} \times 100 \quad (2)$$

where

$C$  = ratio of compressor inlet radius to ring radius

$i$  = number of ring

$\theta^-$  = largest continuous arc of the ring over which the total pressure is below the ring average pressure

$P_{t \max}$  = ring maximum total pressure

$P_{t \text{av}}$  = ring average total pressure

$P_{t \min}$  = ring minimum total pressure

In this specific effort a flight test F-111A aircraft was utilized to determine the dynamic nature of inlet pressure fluctuations related to engine operational stability. Derived steady-state flow distortion patterns as developed from low response pressure instrumentation were compared with both the  $K_{DA}$  and  $K_{DM}$  distortion parameters calculated from high response instrumentation. A typical comparison is shown in Figure 9 for the flight case of Mach number 1.6 at an altitude of 45,000 feet with off-design inlet spike position. Here it is clearly seen that the low response data technique functioning at a sampling rate of 50 cuts per second did not yield information indicative of the compressor stall. On the other hand, utilizing the higher response data technique and calculating either the  $K_{DA}$  or  $K_{DM}$  distortion parameter at 400

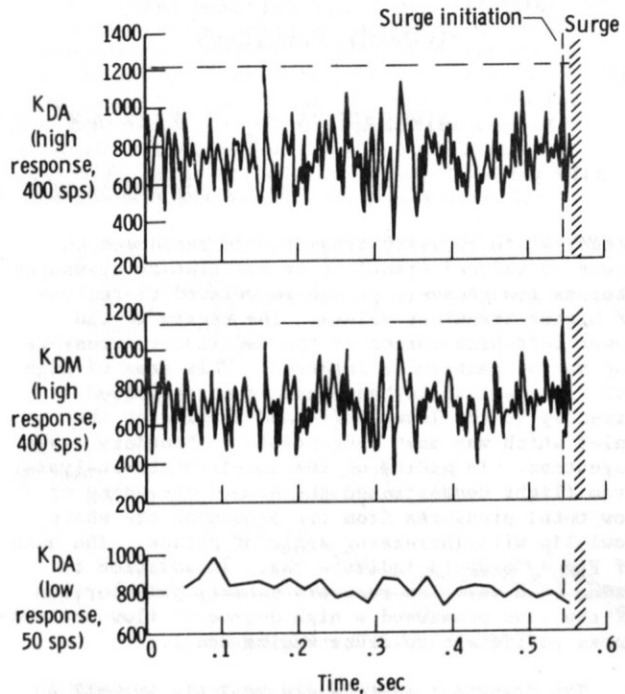


FIGURE 9. COMPARISON OF HIGH AND LOW RESPONSE  $K_{DA}$  WITH HIGH RESPONSE  $K_{DM}$ . F-111A FLIGHT CONDITIONS; MACH NUMBER = 1.6, ALTITUDE = 45,000 FEET AND OFF-DESIGN SPIKE POSITION



samples per second did yield a substantial peak approximately 15 milliseconds prior to surge. Figure 10 shows a time history of the probe data and distortion factor for Mach number 2.17 and an altitude of 44,000 feet. Probes A and B show increases in pressure as the stall condition is approached whereas probes A<sup>1</sup> and B<sup>1</sup> are decreasing and hence result in a maximum distortion value. It is interesting to note that the instantaneous pressure recovery map shows a larger high pressure area along with a more intense low pressure area.

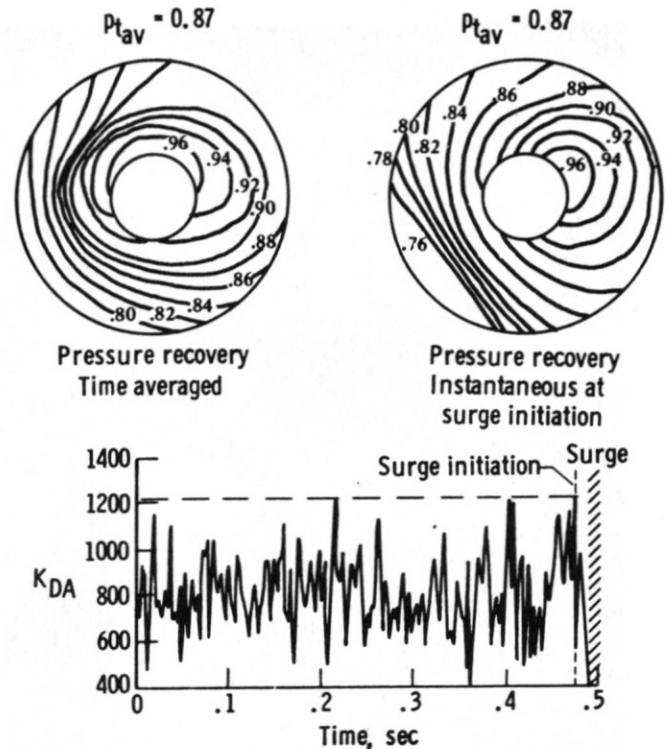
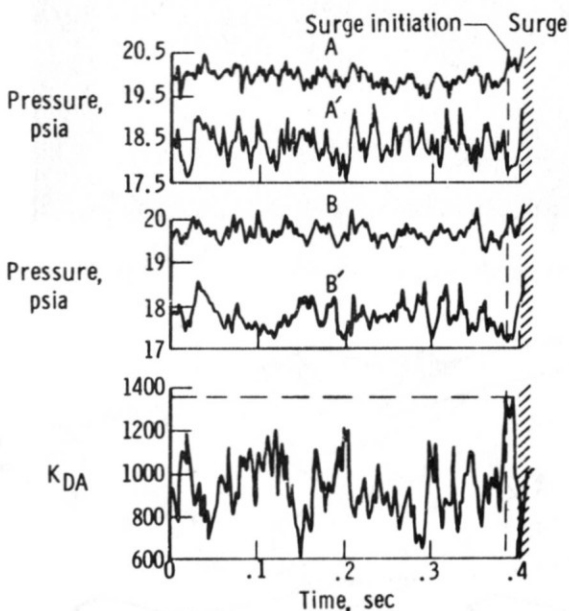
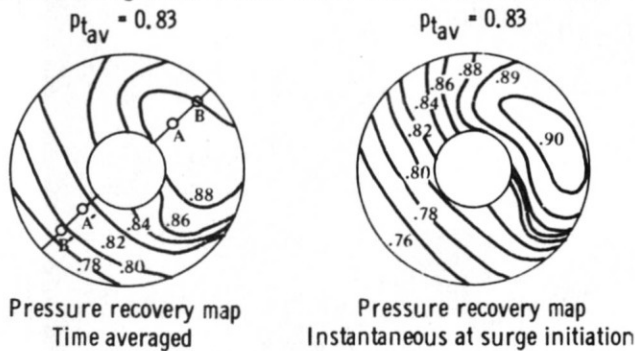


FIGURE 10. COMPARISON OF AVERAGE RECOVERY AND INSTANTANEOUS RECOVERY MAPS WITH  $K_{DA}$ . F-111A FLIGHT CONDITIONS; MACH NUMBER = 2.17, ALTITUDE = 44,000 FEET

Figure 11 shows the surge characteristics for transonic flight at Mach number 0.9 and 30,000 feet altitude. This particular stall occurred as a result of the off-design conditions of the inlet cone and is generally recognized as a "drift" type of surge. This is demonstrated by the fact that peak values of the distortion factor occurred several times during the time period examined.

The modified distortion parameter as developed by Burcham and Hughes<sup>(8)</sup> was found to be approximately 80 percent effective in identifying surge when dynamic conditions prevailed within approximately 90 percent of the maximum steady state distortion value. Needless to say, additional information<sup>(9,10)</sup> and more exacting methods must be developed to predict engine instability due to dynamic inlet conditions.

FIGURE 11. COMPARISON OF AVERAGE RECOVERY AND INSTANTANEOUS RECOVERY MAPS WITH  $K_{DA}$ . F-111A FLIGHT CONDITIONS; MACH NUMBER = 0.9, ALTITUDE = 30,000 FEET AND OFF-DESIGN SPIKE POSITION

#### V. Advanced Inlet Configuration Studies

More recently the Air Force Flight Dynamics Laboratory has undertaken a number of programs to investigate flows about fuselage and wing-fuselage combinations throughout the subsonic, transonic and supersonic speed regimes. The objectives of these programs are to develop a clear understanding of inlet-airframe interactions and, more importantly, to attain an experimental data bank and corresponding analytical approach for assessing the dynamic phenomena associated with engines and inlets. The Laboratory has initiated project Tailor-Mate in order to examine the effects of configuration variations on flow field dynamics and related effects to the engine system. Figures 12 and 13 show a typical 1/3 scale wind tunnel model along with various aircraft configurations studied. Configurations A-1 and A-2 are examples of side mounted type inlets whereas A-3 is an example of a fuselage shielded inlet, and wing shielded inlets are shown by configurations B-3 and B-4. One quarter scale fuselage models were constructed for wind tunnel testing purposes with appropriate fuselage static pressure distributions, boundary layer measurements and more importantly, the dynamic nature of the flow fields at the proposed inlet stations. In addition to the flow field measurements made in the area of the entrance to the inlet, two side mounted and two shielded external compression inlets were tailored for the flow fields defined by the forebody as shown in Figure 14. The detailed instrumentation for such a duct system is shown in Figure 15. Instrumentation was utilized to document the inlet performance and included static pressure rakes near the cowl lip, in the diffuser and at the

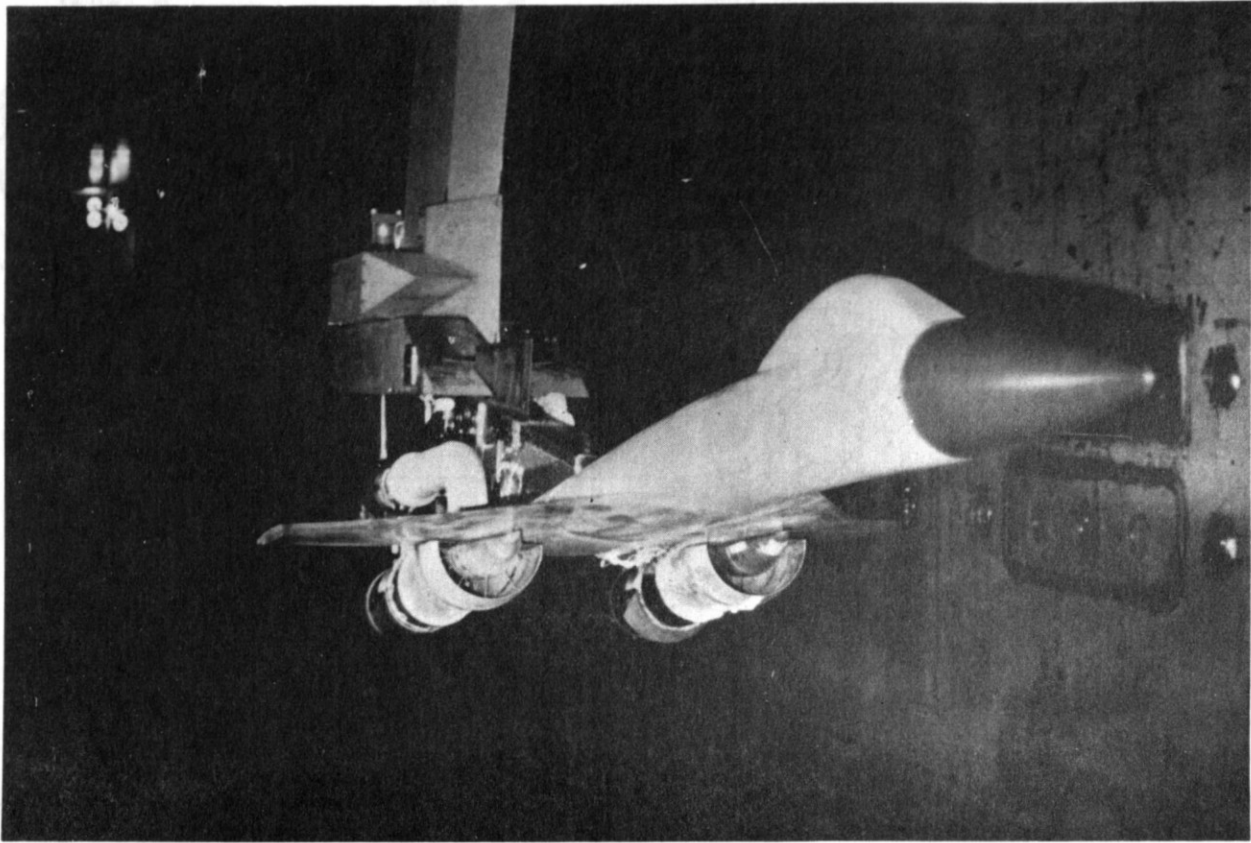


FIGURE 12. TYPICAL 1/3 SCALE TAILOR-MATE WIND TUNNEL MODEL

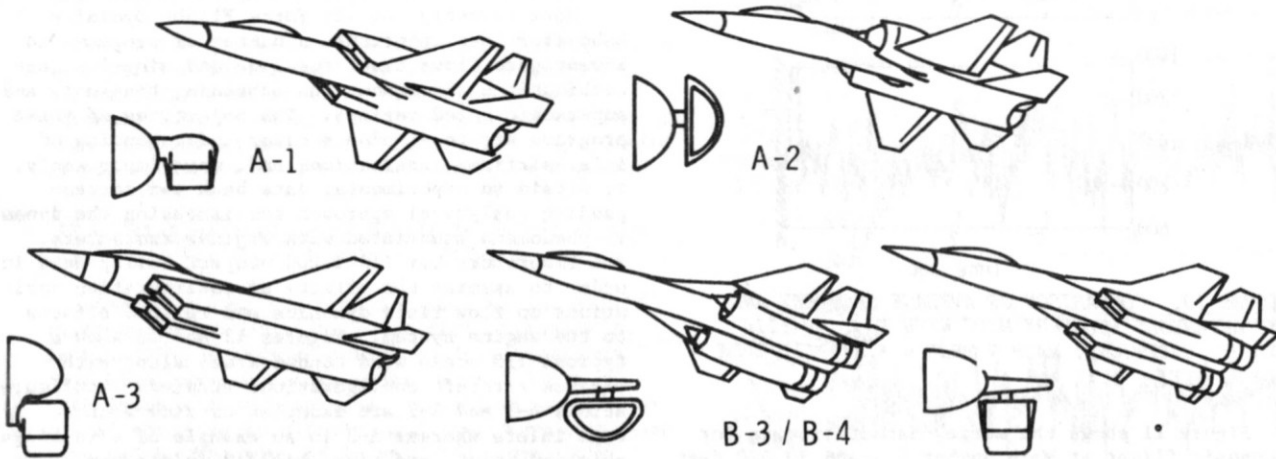


FIGURE 13. REPRESENTATIVE CONFIGURATIONS FOR FOREBODY FLOW FIELD TESTS

simulated compressor face. It is important to note that the compressor face instrumentation contained high response type transducers to identify the fluctuation nature of the inlet flow. Figure 16 shows the results of wind tunnel tests for the four configurations mentioned. These tests were performed at Mach number 2.2 with varying angle of attack. Figure 16 shows both wing shielded inlet systems experienced lower distortion as indicated by the simple distortion index along with low "turbulence" as a function of angle of attack. As might be expected the side mounted type of inlets

experienced higher distortion with correspondingly higher indices of "turbulence."

The importance of the flow field generated by the forebody of the fuselage has been pointed out by Surber and Stava<sup>(11)</sup> and Zonars<sup>(12)</sup>. An example of such sensitivity is shown in Figure 17 wherein the side mounted 2-dimensional inlet on body A-1 was examined in conjunction with body A-2. This figure shows the vastly different characteristic of distortion vs "turbulence." Surprisingly enough, the small change in contour of the A-2

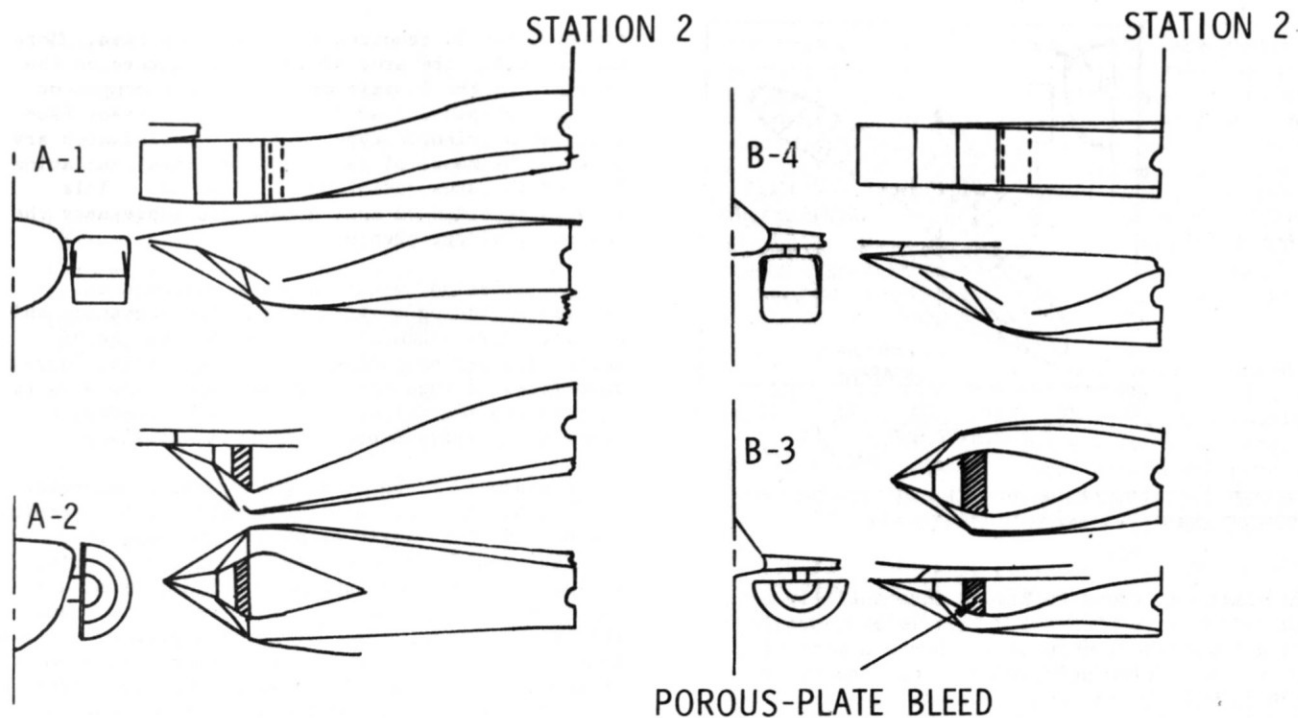


FIGURE 14. NOMENCLATURE AND COMPARISON OF FOUR (4) INLET DESIGNS

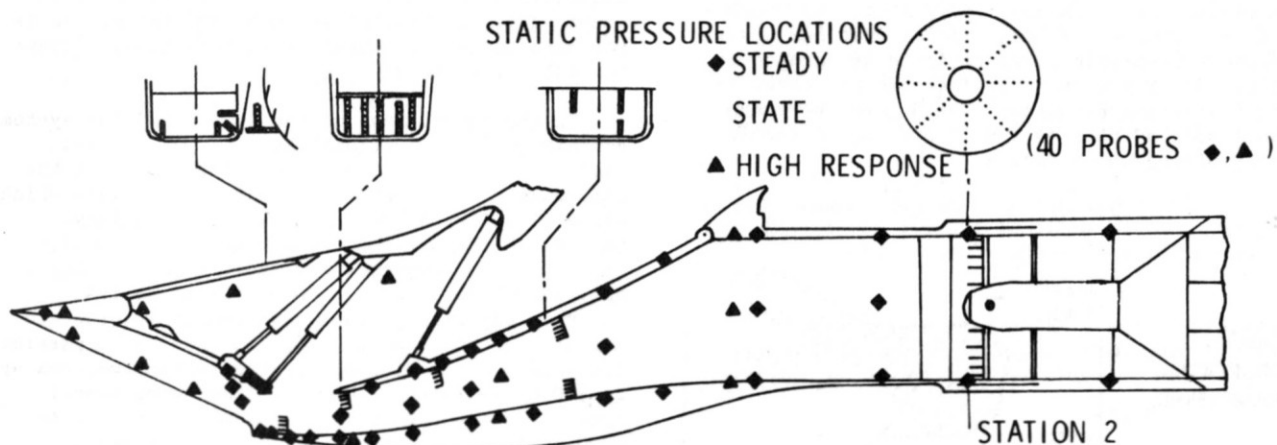


FIGURE 15. TYPICAL INLET INSTRUMENTATION

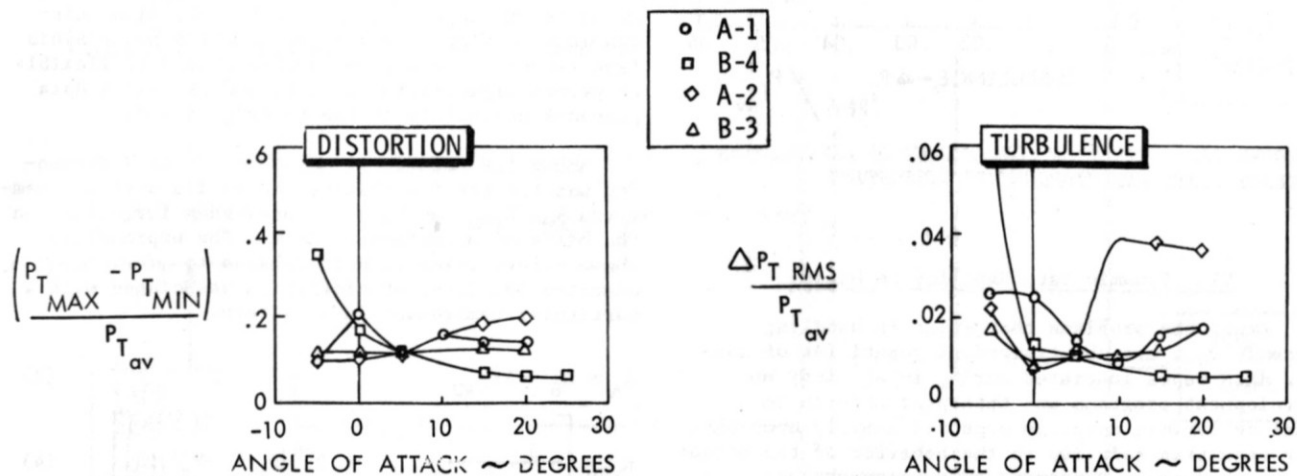


FIGURE 16. COMPARISON OF STEADY-STATE AND DYNAMIC DISTORTION FOR VARIOUS CONFIGURATIONS AT MACH NUMBER 2.2

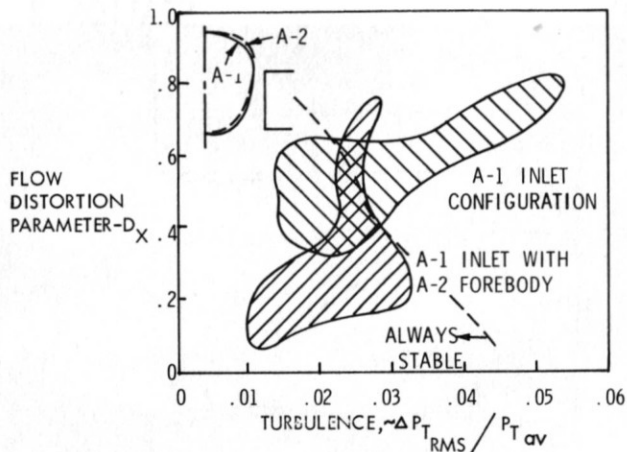


FIGURE 17. INFLUENCE OF FOREBODY CONTOUR ON ENGINE STABILITY AT MACH NUMBER 2.2

fuselage was found to have a substantially better characteristic than A-1. This is undoubtedly due to a lower local outwash and hence a reduced tendency toward flow separation on the inboard side of the inlet. In the event the designer is confined to the A-1 inlet configuration and cannot readjust the body contour as shown by the A-2 characteristics, he must then look for other means by which he can suppress both the steady state and "turbulent" distortion. A longer inlet duct has a surprisingly favorable characteristic as denoted in Figure 18. There is a considerable reduction in both distortion parameters which puts the operational mode of the inlet well within the stable bounds of engine operation.

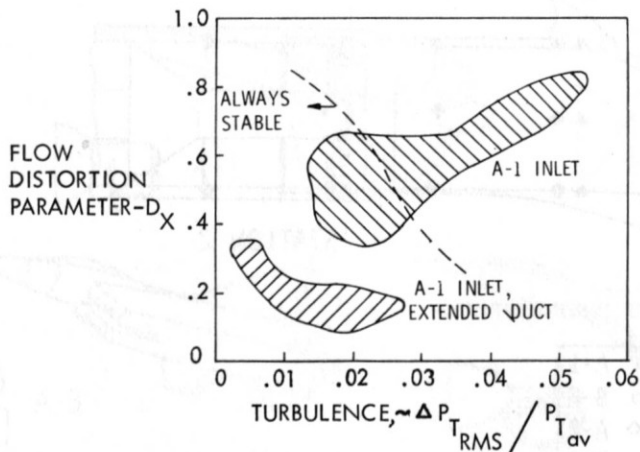


FIGURE 18. EFFECT OF LONGER DUCT ON SUPPRESSING STEADY STATE AND "TURBULENT" DISTORTION

## VI. Dynamic Data Handling Technique

Among the problems that exist in handling dynamic data are the tremendous quantities of analog data tapes generated during inlet study and development programs and that past efforts to analyze dynamic data has depended heavily upon what has been seen relative to the behavior of the steady state or average component of compressor face total pressure. As a consequence, only about one percent of the data is actually examined since considerable

digitization is required to review one case. More specifically, the area of interest centers on the analysis of the dynamic or fluctuating component of total pressure measured at the compressor face plane of a trisonic type inlet. The pressures are measured by means of fast response instrumentation located in rakes radiating from the hub. This data is recorded on analog tape and represents the beginning of our problem.

The solution to this problem has been to develop an analog editing system for screening and editing inlet dynamic data based on the use of engine distortion parameters. As a result, large quantities of tape can be screened and those parts of the data identified which would have adverse effects on airframe-propulsion compatibility.

A typical Air Force Flight Dynamics Laboratory inlet program consists of 5000 data points wherein one Mach number, angle of attack and yaw, and capture area ratio comprises a single data point. At least 200 feet of tape are used for each data point and as a result, it can be seen that about 100 reels of tape are required for a program of this magnitude. For a more extensive inlet development program, such as associated with advanced flight vehicles, as many as 500 tapes are required. In any event, the data of interest is contained on only about one percent of the tape which is not necessarily the same one percent of tape mentioned previously. The principle question that arises is how does one expeditiously and economically locate the data of interest?

In the development of the analog editing system, certain goals were established. First, it was desirable to utilize parameters involving all the compressor face steady-state and dynamic data which had a direct relationship to engine stability. Second, a scheme was desired that would identify high levels of dynamic flow activity on the tapes and where this event occurred. Third, a fast response capability was a requirement in order to account for model scale. For example, if a particular engine is sensitive to pressure fluctuations up to 200 cycles/second, and the inlet wind tunnel model is one-tenth scale, then valid data out to 2000 cycles/second is required from the model. Model scaling characteristics have been hypothesized by Sherman and Motycka<sup>(13)</sup>. Fourth, a desirous capability was to use more than one parameter in the screening process to determine which was most meaningful and acceptable and hence avoid tape re-runs. Fifth, the system should be flexible to permit digitization of data and possess a data playback capability at the recorded speed.

Among the parameters selected for data screening was the Pratt & Whitney engine distortion parameters  $K_\theta$ ,  $K_{RAD}$  and  $K_A$  which have been formulated on the basis of experimental data. The expressions shown below, which in part relates to reference (12), describe the level of distortion associated with a particular compressor face pattern.

$$K_A = K_\theta + bK_{RAD} \quad (3)$$

$$K_{RAD} = \left[ \frac{1}{Q_{av} \sum_{i=1}^i D_i^{-x}} \right] \sum_{i=1}^i \left[ D_i^{-x} \left( P_{t_{av}} - P_{t_{av}, i} \right) \right] \quad (4)$$

where

b = constant depending on engine design and entrance Mach number

x = weighting factor depending on distortion sensitivity

$K_{\theta}$  describes the influences associated with a circumferential distortion pattern while  $K_{RAD}$  describes the pattern variation associated with radial distortion. When a combined pattern exists, which is typically the case,  $K_{\theta}$  and  $K_{RAD}$  are added together in a weighted manner to form  $K_A$ . In addition to the Pratt and Whitney parameters, a set of General Electric engine distortion parameters have been programmed. These expressions are used to identify high levels of dynamic activity in the air flow process. These data are subsequently subjected to further analysis which in turn aids in determining the necessary modifications required to alleviate the compatibility problem.

The dynamic data screening device or system was developed jointly between the Air Force Flight Dynamics Laboratory and the Aeronautical Systems Division Computer Center using a hybrid computer. This program was initiated in January 1970 by Sedlock and Marous<sup>(14)</sup> with the acquisition of a 72 channel multiplex discriminator system, a 14 track direct playback tape transport, tape search unit peak detectors, and a 48 channel data filtering system. The complete system shown in Figure 19 became operational in July 1971. The system described above is similar to that developed by Crites and Heckart<sup>(15)</sup>, Crites<sup>(16)</sup>, Lynch and Slade<sup>(17)</sup> except for the added flexibility due to a hybrid computer capability.

The current status of the Air Force Flight Dynamics Laboratory system is that both General Electric and Pratt and Whitney engine distortion parameters have been programmed on the computer and up to five parameters can be tracked simultaneously with an order of priority established for each parameter. The primary requirement of the system is to identify dynamic peaks and the time of

occurrence. The resolution of the tape search unit permits identification of the peak value within one millisecond. Center frequencies used in the discriminators have been selected for greatest compatibility with those being used by USAF and contractor facilities. The dynamic data can be filtered from 125 to 9000 cycles/second in six discrete increments in order to account for model scale and filtering of any unwanted high frequency information such as probe resonance. Both the engine distortion parameters and pressure data can be digitized at various sampling rates.

Our past and current efforts have included review of the compatibility points in the B-1 Interface Control Document and the Arnold Engineering Development Center 1/10 scale inlet test data. In addition to continued support of the B-1 program, data from the RA-5C wind tunnel-flight test correlation and Tailor-Mate programs will be reviewed.

McDonnell-Douglas personnel<sup>(16)</sup> have developed a screening system for use during the F-15 inlet development program. In examining this capability to review dynamic data based on conventional means, it was estimated that six man-years and one million dollars were required to review one percent of a 250 data point program which represented some four million pressure distributions. The development of an analog editing system reduced this task to six weeks with less than 1000 feet of tape to be examined. Our own experience has shown that one reel of tape containing 30 data points can be examined in approximately one hour. To accomplish the same task with a digital computer would require 15 hours to digitize the data and approximately 20 hours of computer time to process the information. This estimate is based on 200 samples per data point. The development described above represents a major step in handling the extremely large amount of data associated with an inlet development program.

A description of how the engine distortion are implemented on the analog/digital computer to accomplish the goal of editing and screening the

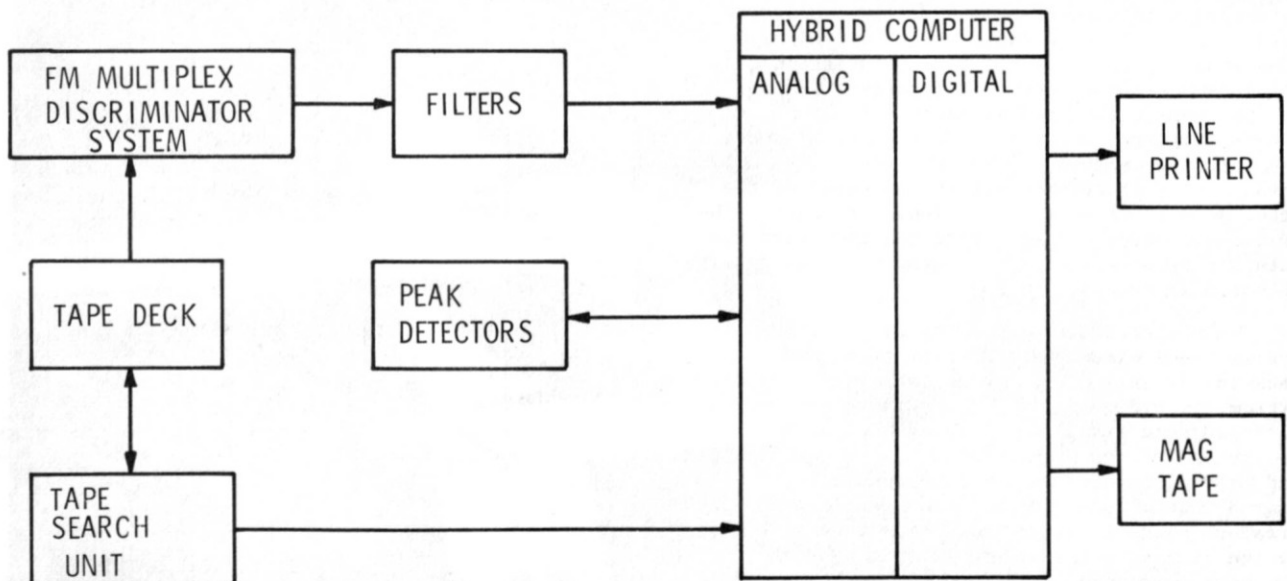


FIGURE 19. DYNAMIC DATA SCREENING AND EDITING SYSTEM

data will now be addressed. This can be accomplished by relating the expression for  $K_{\theta}$  to a particular configuration of total pressure probes at the compressor face. In this particular case, consider a configuration that consists of 48 probes with six rings and eight rakes. The implementation of Equation (3) on the analog computer is quite simple. The steady-state and gain adjusted fluctuating pressure are summed together to form the total component of pressure. Each pressure is multiplied by its respective  $\sin\theta$  and  $\cos\theta$ , summed around each ring, and then squared. These two terms are added together and then the square root is taken of this summation. Finally, this value is multiplied by the value of the leading term to attain  $K_{\theta}$  for one ring. This process is repeated for each ring and then the individual ring  $K_{\theta}$  are summed together to form the total  $K_{\theta}$ . While the value of this expression is being calculated, a similar process is occurring simultaneously for the other parameters.

The editing process is accomplished by considering the time history of the parameter  $K_{\theta}$ ,  $K_{\theta}$  can be generated as a continuous function since an analog computer is a continuous type of machine. The operator has the ability to set a threshold level for each of the parameters such that only information occurring about that level will be examined. The engineer must know when a peak in  $K_{\theta}$  has been experienced and the time of this occurrence. In addition, he is interested in the value of  $K_{\theta}$  when it exceeds a given threshold level and when it returns to a lower value. Special peak detector networks are utilized to accomplish these objectives. These peak detectors track an increasing signal to the peak level and maintain that level until it is reset. The peak detectors are normally reset when the value of the parameter drops below the threshold level in order that successive peaks can be detected even though such peaks may be of a lower value than a preceding peak. In addition, the peak detectors can be used as a signal generator that signifies a peak has been detected. Judgement must be made as to identifying both threshold crossings and peaks or peak values alone. When a threshold crossing occurs, an interrupt signal is generated, and the information is transferred from the analog to the digital computer. No on-line manipulation of this information is permitted in order to transfer the data as quickly as possible. The current response time from signal interrupt thru information transfer is 300 microseconds. An important feature of the program is the identification of which parameters triggered the interrupt signal. Whenever the interrupt signal occurs, the peak value of the parameter is stored as well as the value of the other parameters at this particular instant. The next output from the editor is the time when the peak was detected. The time resolution is to within one millisecond.

Many electronic components make up the editing system. A 14 track tape transport is used to playback the dynamic data through the discriminator system which de-multiplexes the individual signals. Each pressure signal is filtered before it is sent to the analog computer. Coupled with the tape deck and hybrid computer is the tape search unit. The search unit allows one to find a particular time-pressure history on the tape while it also serves as the time reference frame for the hybrid computer. The peak detectors, mentioned earlier, are coupled to the analog computer. The information stored in the digital computer can be printed out on the

line printer or stored on magnetic tape.

## VII. Advanced Nozzle Configuration Studies

The Air Force Flight Dynamics Laboratory has undertaken a number of programs<sup>(18)</sup> to investigate the effects of airframe-nozzle interactions throughout the subsonic, transonic and supersonic speed regimes. The objective of these programs is to develop a clear understanding of nozzle-airframe interactions and hence improve the technology base. A basic aircraft configuration incorporating a common forebody, wing, inlet system, and a twin engine installation shown in Figure 20, was utilized during high Reynolds number ( $0.5 - 6 \times 10^6$  per foot) wind tunnel tests to determine the relative merits of a

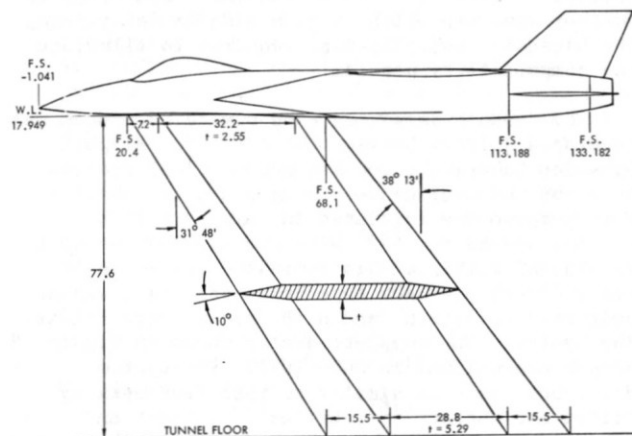


FIGURE 20. BASIC TWIN-ENGINE WIND TUNNEL MODEL; ALL DIMENSIONS IN INCHES

wide spectrum of aft-body nozzle geometrical variations. This figure shows a schematic of the model and the support system required to conduct tests in the 16 foot AEDC Propulsion Transonic and Supersonic Wind Tunnels. Cross-sectional area distributions, including the influence of the support strut system and the effect of nozzle spacing, is shown in Figure 21.

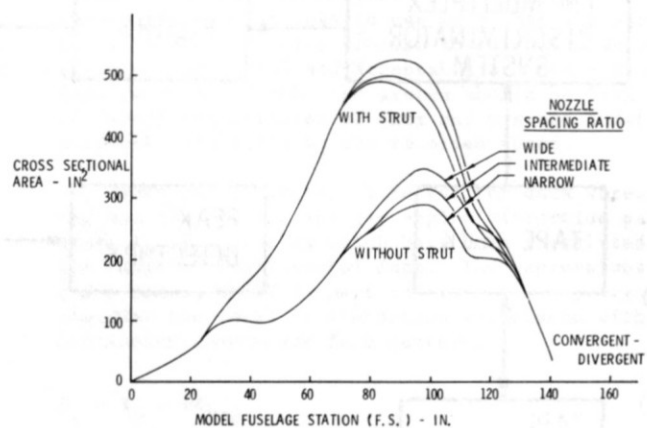


FIGURE 21. WIND TUNNEL MODEL AND SUPPORT SYSTEM CROSS-SECTIONAL AREA CHARACTERISTICS  
The same type of area distributions, involving the

effect of wing, tail and the limits of nozzle setting, are shown in Figure 22. The various nozzles,

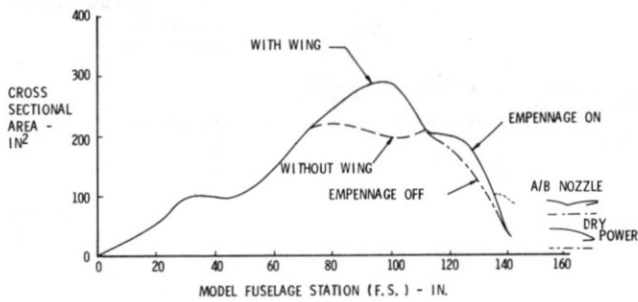


FIGURE 22. WIND TUNNEL MODEL CROSS-SECTIONAL AREA CHARACTERISTICS

which were connected or disconnected at fuselage station 133.182 inches for non-afterburning conditions are shown in Figure 23. Maximum afterburning

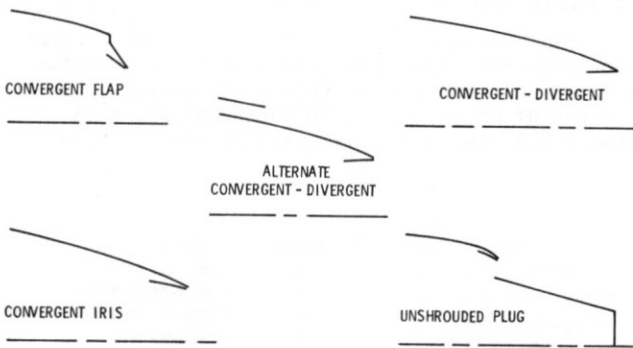


FIGURE 23. SYSTEM OF NON-AFTERBURNING NOZZLES CONFIGURATIONS TESTED

nozzle contours are shown in Figure 24 and were similarly attached to the same fuselage location. The large scale wind tunnel model shown in Figure

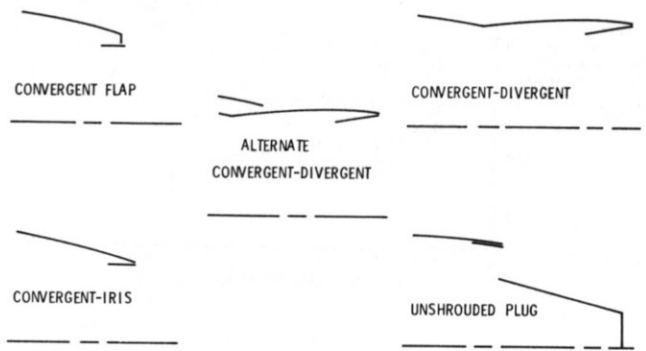


FIGURE 24. AFTERBURNING NOZZLE CONFIGURATIONS TESTED

25 was configured in such a manner as to employ a system of balances which measured both the aft-body boattail drag and the nozzle boattail drag. In addition, a thrust balance was incorporated to measure the internal thrust and nozzle boattail drag. It is important to note that both the horizontal and vertical tail were not included in the drag measurements aforementioned.

The nozzle boattail drag characteristics for the non-afterburning condition is shown in Figure 26 for Mach number 0.9. The drag coefficients displayed in this figure are referenced to the cross-sectional area located at fuselage station 133.182 inches. The convergent-divergent and convergent iris nozzles, which are basically slender in nature,

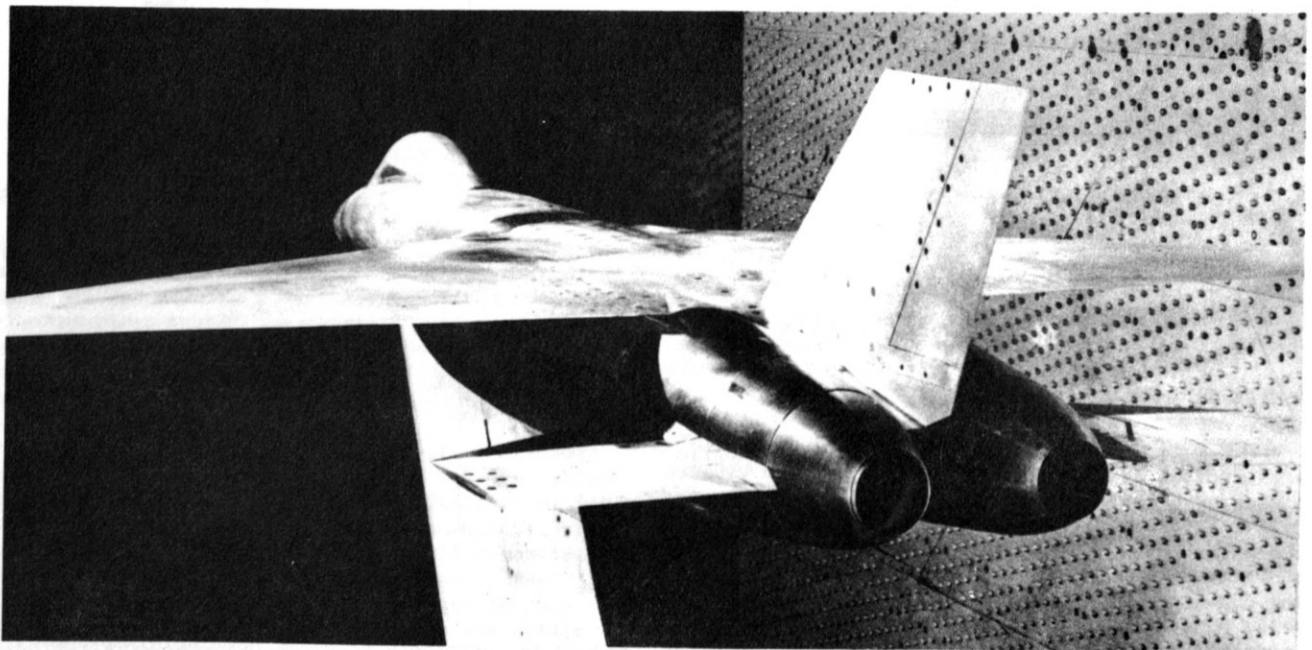


FIGURE 25. PHOTOGRAPH OF MODEL INSTALLED IN THE 16 FOOT AEDC TRANSONIC PROPULSION WIND TUNNEL

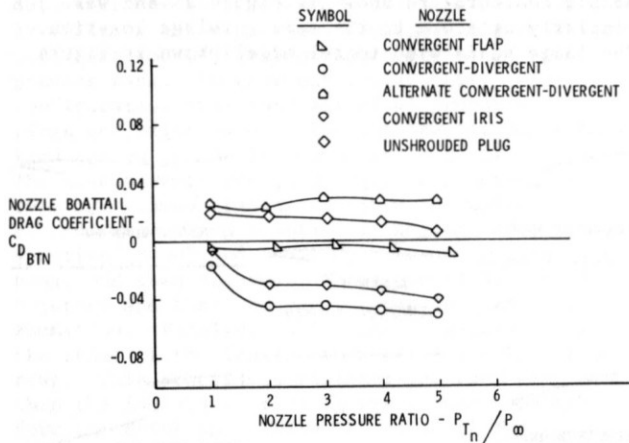


FIGURE 26. NON-AFTERBURNING NOZZLE BOATTAIL DRAG CHARACTERISTICS; MACH NUMBER = 0.9

displayed the lowest drag characteristics. In fact, these two nozzles, along with the convergent flap nozzle, experienced pressurization of the external aft-facing surfaces and, hence, were subjected to a thrust rather than a drag force. The alternate convergent-divergent nozzle experienced the highest drag due to flow separation caused by the rearward facing step between the nozzle and fuselage fairing. The unshrouded plug nozzle also experienced separated flow, which basically prevented pressurization of the external surfaces with correspondingly lower relative drag.

The nozzle boattail drag based on maximum afterburner nozzle position for Mach number 0.9 is shown in Figure 27. The convergent-flap and convergent-iris nozzles show good pressure recovery

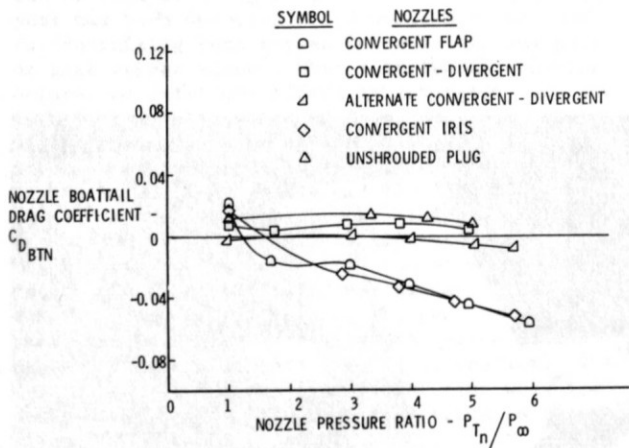


FIGURE 27. AFTERBURNING NOZZLE BOATTAIL DRAG CHARACTERISTICS; MACH NUMBER = 0.9

characteristics, particularly with increased nozzle pressure ratio. The remaining three nozzles yielded higher drag characteristics. The same nozzle boattail drag characteristics associated with the maximum afterburner position for Mach number 1.2 is shown in Figure 28. Here it can clearly be seen that the convergent-flap and convergent-iris nozzles involve a substantial drag penalty due to the large projected frontal area; however, the drag coefficient of these two nozzles diminishes with increased pressure ratio as might be expected with a Mach number

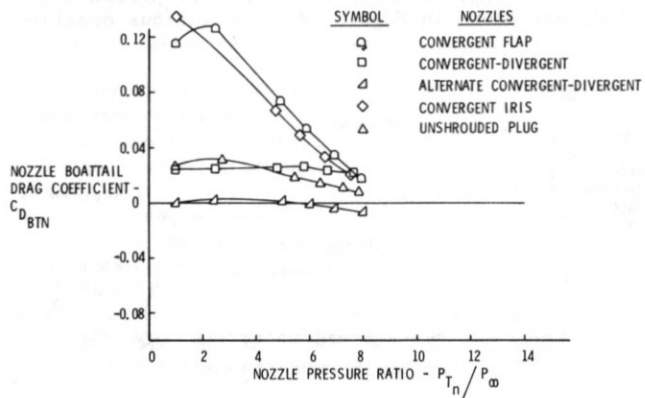


FIGURE 28. AFTER-BURNING NOZZLE BOATTAIL DRAG CHARACTERISTICS; MACH NUMBER = 1.2

1.2 flight requirement. The convergent-divergent and unshrouded-plug nozzles have lower drag characteristics than the two aforementioned nozzles primarily due to the reduced aft-facing surface areas. The alternate convergent-divergent nozzle displayed the best characteristics with very little influence of nozzle exhaust pluming effects.

The aft-body boattail drag coefficient, based upon the cross-sectional area at fuselage station 113.188 associated with the non-afterburning nozzle and afterburning nozzle positions for Mach number 0.9, is shown in Figures 29 and 30. The

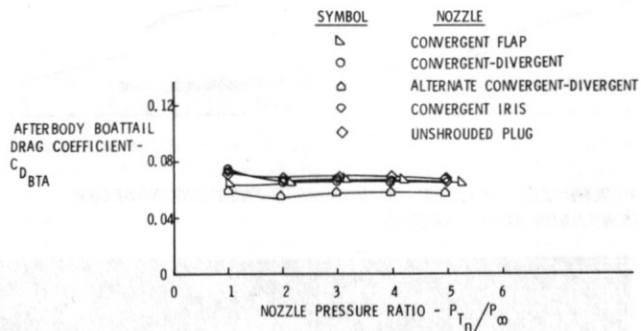


FIGURE 29. AFT-BODY BOATTAIL DRAG CHARACTERISTICS; NON-AFTERBURNING NOZZLES, MACH NUMBER = 0.9

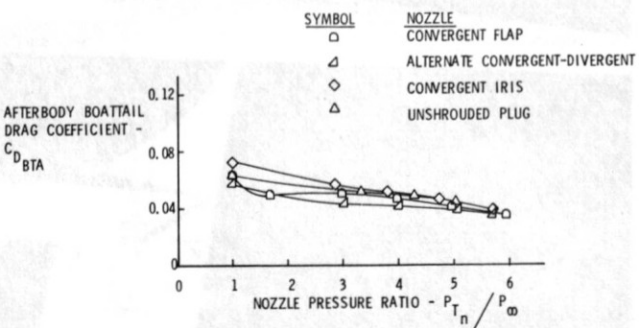


FIGURE 30. AFT-BODY BOATTAIL DRAG CHARACTERISTICS; AFTERBURNING NOZZLES, MACH NUMBER = 0.9



same aerodynamic coefficient for Mach number 1.6 with maximum afterburner nozzle conditions is shown in Figure 31. In all three cases, the afterbody

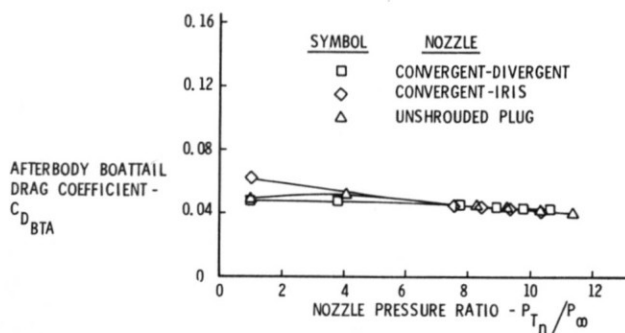


FIGURE 31. AFT-BODY BOATTAIL DRAG CHARACTERISTICS; AFTERBURNING NOZZLES, MACH NUMBER = 1.6

boattail drag was of a positive nature with small differences caused by downstream changes in the nozzle boattail geometry.

The total drag coefficient, i.e., the summation of aft-body boattail drag and nozzle boattail drag, is shown in Figure 32. Here we see that the

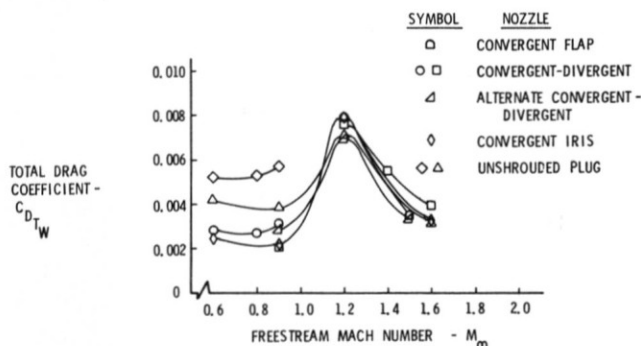


FIGURE 32. TOTAL AFT-END DRAG CHARACTERISTICS

total aft-end drag variations based upon aircraft wing area is principally due to aft-body boattail drag characteristics previously described. Also, one can observe that the total aft-end drag is of a positive nature mainly due to the aft-body boattail section. Variations of this drag are associated with the nozzle boattail drag characteristics.

Reynolds number effects on the total aft-body drag are shown in Figure 33. These results, which show increasing aft-body drag as a function of increasing unit Reynolds number, was unexpected since skin friction effects and separated flow conditions normally improve such circumstances with lower resulting drag. Although not presented in this paper, the Reynolds number effects on the nozzle boattail drag were of an opposite nature.

The nozzle test characteristics and results presented above represent a complex interaction between external and internal flows. The issue is further clouded by viscous considerations. The accurate simulation of all important parameters is very difficult, even to the point where some parameters are not fully defined or identified. A research and development effort is required to define the proper parameters and their associated importance.

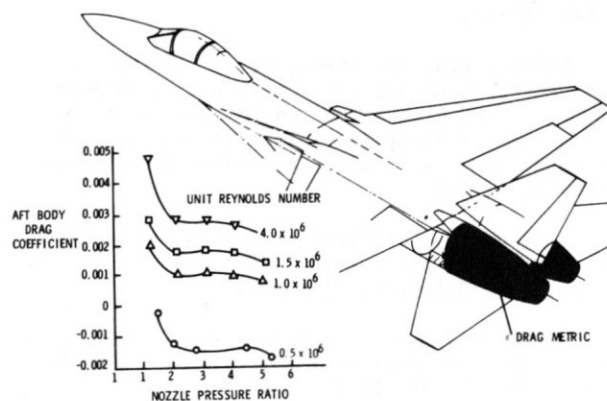


FIGURE 33. AFT-BODY DRAG CHARACTERISTICS AS A FUNCTION OF REYNOLDS NUMBER; MACH NUMBER = 0.9

#### REFERENCES

1. Gabriel, D.S., Wallner, L.E., and Lubick, R.J., "Some Effects of Transients in Inlet Pressures and Temperatures on a Turbojet Engine," Institute of the Aeronautical Sciences Twenty-Fifth Annual Meeting, (January 1957).
2. Martin, A.W. and Kostin, L.C., "Propulsion System Dynamic Test Results," North American Aviation, Inc., Report No. NA-67-386, (April 1967).
3. Winslow, L.J., et. al., "Inlet Distortion Investigation, Upstream Engine Influence and Screen Simulation," The Boeing Company, Technical Report AFAPL-TR-68-140, (January 1969).
4. Wasserbauer, J.F. and Willoh, R.G., "Experimental and Analytical Investigation of the Dynamic Response of a Supersonic Mixed Compression Inlet," AIAA Preprint 68-651 (1968).
5. Martin, A. and Kostin, L., "Dynamic Distortion at the Exit of a Subsonic Diffuser of a Mixed Compression Inlet," North American Rockwell, Report TFD-69-588 (1969).
6. Oates, G.C., Sherman, D.A., Motycka, D.L., "Experimental Study of Inlet-Generated Pressure Fluctuations," PWA Report 3682 (1969).
7. Plourde, G.A. and Brimelow, B., "Pressure Fluctuations Cause Compressor Instability," Air Force Airframe/Propulsion Compatibility Symposium, (June 1969).

8. Burcham, F.W., Jr. and Hughes, D.L., "Analysis of In-Flight Pressure Fluctuations Leading to Engine Compressor Surge in an F-111A Airplane for Mach Number to 2.17," AIAA Preprint 70-264 (1970).

9. Calogeras, J.E., Burstadt, P.L. and Coltrin, R. E., "Instantaneous and Dynamic Analysis of Supersonic Inlet-Engine Compatibility," AIAA Preprint 71-667 (1971).

10. Jansen, W., "Compressor Sensitivity to Transient and Distorted Transient Flows," AIAA Preprint 71-670 (1971).

11. Surber, L.E. and Stava, D.J., "Supersonic Inlet Performance and Distortion During Maneuvering Flight," AGARD Propulsion and Energetics Panel Specialists' Meeting on "Inlets and Nozzles for Aerospace Engines," AGARD Conference Proceedings CP-91-71, (1971).

12. Zonars, D., "Problems on Inlets and Nozzles," 7th Congress of the International Council of the Aeronautical Sciences, (August 1970).

13. Sherman, D.A., and Motycka, D.L., "Experimental Evaluation of a Hypothesis for Scaling Inlet Turbulence Data," AIAA Preprint 71-669 (1971).

14. Sedlock, D. and Marous, J., private communication, (1972).

15. Crites, R.C. and Heckart, M.V., "Application of Random Data Techniques to Aircraft Inlet Diagnostics," AIAA Preprint 70-597 (1970).

16. Crites, R.C., "The Philosophy of Analog Techniques to the Analysis and High Speed Screening of Dynamic Data," AIAA Preprint 70-595 (1970).

17. Lynch, F.R. and Slade, C.J., "Data Acquisition and Automated Editing Techniques for Engine-Inlet Tests," AIAA Preprint 70-596 (1970).

18. Air Force Flight Dynamics Laboratory, "Experimental and Analytical Determination of Integrated Airframe-Nozzle Performance," Interim Report (1972).